Acta Mechanica Solida Sinica, Vol. 20, No. 3, June, 2008 ISSN 0894-9166
Published by AMSS Press, Wuhan, China. DOI: 10.1007/s10338-008-0823-4

DETERMINATION OF INTERFACIAL MECHANICAL PARAMETERS FOR AN Al/EPOXY/Al_2O_3 SYSTEM BY USING PEEL TEST SIMULATIONS **

Xuemei You Haifeng Zhao Yueguang Wei*[1]

(*State-Key Laboratory of Nonlinear Mechanics, Institute of Mechanics, Chinese Academy of Science, Beijing* 100190*, China*)

Received 26 April 2007; revision received 21 April 2008

ABSTRACT Peel test measurements and simulations of the interfacial mechanical parameters for the Al/Epoxy/Al_2O_3 system are performed in the present investigation. A series of Al film thicknesses between 20 and 250 microns and three peel angles of 90, 135 and 180 degrees are considered. Two types of epoxy adhesives are adopted to obtain both strong and weak interface adhesions. A finite element model with cohesive zone elements is used to identify the interfacial parameters and simulate the peel test process. By simulating and recording normal stress near the crack tip, the separation strength is obtained. Furthermore, the cohesive energy is identified by comparing the simulated steady-state peel force and the experimental result. It is found from the research that both the cohesive energy and the separation strength can be taken as the intrinsic interfacial parameters which are dependent on the thickness of the adhesive layer and independent of the film thickness and peel angle.

KEY WORDS peel test, interface toughness, cohesive zone model, energy release rate

I. INTRODUCTION

Extensive applications of thin film materials have led to wide researches on the strength, ductility and reliability of the thin film/substrate systems in recent years[1–12]. Mechanical behaviors of the thin film/substrate systems were thought to be dominated by their interface adhesion properties which are often characterized by two parameters of both the interfacial toughness and the adhesion strength[4–10]. In this paper we shall focus our attention on the investigation of the interfacial behaviors for thin Al films with thickness ranging between 20 and 250 micrometers bonded to a ceramic substrate (Al_2O_3) by two types of epoxy adhesives. Interfacial energy (or fracture toughness) Γ_0 is an important parameter and is usually measured directly by peel tests[2,3,11–16] when plastic dissipation energy is small. Figure 1 illustrates the configuration of a peel test with the film thickness t, peel force P and peel angle Φ. The

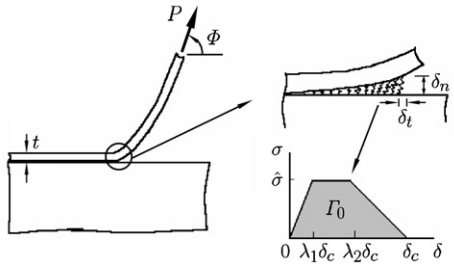

Fig. 1 Peel test configuration and sketch of the cohesive zone model.

* Corresponding author. E-mail: ywei@lnm.imech.ac.cn

** Project supported by the Chinese Academy of Sciences (No.KJCX2-YW-M04) and the National Science Foundation of China (Nos.10432050, 10672163 and 10721202).

right hand part of Fig.1 sketches the cohesive zone (CZ) model by which usually the interface parameters can be described[3–5,8–10,16,17]. From Fig.1 another important interface parameter, the separation strength $\hat{\sigma}$, has been defined. Through the peel test one can record the peel force P and the deformation information of the film. From energy balance at the steady-state peeling process, the energy release rate (or peel force P) comprises not only the fracture toughness Γ_0 but also the plastic dissipation energy Γ_P,

$$P(1-\cos\Phi) = \Gamma_0 + \Gamma_P \tag{1}$$

where Φ is the peel angle. In most metal film cases Γ_P is a major contribution to the total energy release rate $P(1-\cos\Phi)$. So an appropriate method is needed to determine Γ_0 from Eq.(1)[1,3,8–10,15,18–23].

Kim et al.[18,20] presented an elastic-plastic beam bending model to estimate the plastic dissipation Γ_P. Wei[4,5] and Wei and Hutchinson[17] presented a plane strain elastic-plastic analysis model with the cohesive zone (CZ) to model the plastic dissipation energy. In Wei-Hutchinson model, they combined the beam bending model with the plane strain finite element (FE) calculation. Wei and Zhao[24] investigated the effectiveness of several analytical models by comparing the predicted results of analytical models with the results of peeling experiments, and they concluded that the beam bending model was only suitable for large film thickness case, while Wei-Hutchinson model was suitable for both large and small film thickness cases. The difference of length scales can be described by the magnitude of a nondimensional parameter t/R_0, where t is the film thickness and

$$R_0 = \frac{\dfrac{\hat{\sigma}}{\sigma_Y}\dfrac{E}{\sigma_Y}\delta_c}{3\pi(1-\nu^2)} \tag{2}$$

is plastic zone size near crack tip in the film in the small scale yielding case. $\delta_c = (\delta_n^{c\,2} + \delta_t^{c\,2})^{1/2}$ is another important parameter in the CZ model, and can be expressed by Γ_0 and $\hat{\sigma}$; E, ν and σ_Y are Young's modulus, Poisson's ratio and yield stress of the film, respectively. Zhao and Wei[25] studied the interface properties of the micron-thick metal film along the ceramic substrate without an adhesive layer between film and substrate by using the neural network method, and they also investigated the interface properties of the metal film along the ceramic substrate with a ductile adhesive layer between film and the substrate by using the neural network method[26].

In this paper we shall use the peel test finite element simulations to determine the interface properties of the metal film along the ceramic substrate with an adhesive layer between film and substrate. Peel test measurements of the energy release rates are performed. Three cases of peel angles 90, 135 and 180 degrees are considered. Two types of epoxy adhesives (ductile and brittle adhesives) to bond the Al thin film with thickness ranging between 20 and 250 micrometers to Al_2O_3 substrate are taken into consideration. A rigorous plane strain FE model with the cohesive zone elements is adopted to simulate the peel test process. A detailed procedure to identify the fracture toughness Γ_0 and separation strength $\hat{\sigma}$ is shown. With the experimental stress-strain curves of the adhesives, we obtained the cohesive strength by simulating and recording the near-tip normal stress. Furthermore, the cohesive energy Γ_0 is identified by comparing the simulated peel force with the experimental result. It is found that once these two parameters are determined for one film thickness and one peel angle, the FE model can be used without further modification of the two parameters to predict the results of peel tests with other film thicknesses and peel angles. The cohesive energy Γ_0 is an intrinsic interfacial parameter which is independent of the film thickness and peel angle. But Γ_0 is dependent on the thickness of the adhesive layer. The constraint effect of the adhesive layer thickness is also discussed in this paper.

II. EXPERIMENTS

A series of peel tests are performed to investigate the effect of the film thickness, peel angle and adhesive layer thickness on the peel force.

2.1. Experiment Review

Flexible-rigid peel tests are performed using the series of the Al film thickness, 20, 50, 80, 100, 200, 225 and 250 microns bonded to 4.5 mm thick Al_2O_3 substrates with two types of epoxy/polyimide paste adhesives. Two mass ratios of epoxy/polyimide in the adhesives, 1.5 and 1.0, are adopted. The

first adhesive (ratio 1.5) shows ductile property (limit strain is about 56%) and the second adhesive (ratio 1.0) shows brittle property (limit strain is about 8.7%). Due to the high Young's modulus of the material Al_2O_3, the substrates can be treated as rigid in finite element simulations.

It is crucial to control the adhesive layer thickness d in preparing samples. In our peel tests the adhesive layer thickness is kept constant by adding some small SiO_2 spheres to the adhesive (volume fraction of SiO_2 spheres $< 3\%$). Without specification the adhesive layer thickness is 20 micrometers in the present paper.

All the peel tests are performed using a standard tensile testing machine with a small-scale peel test rig made specifically for the current research (see Fig.2). Several peel angles can be easily maintained with this peel test rig. A Questar measuring microscope with long focus is used to observe the crack growth and take micrographs. The thin films are difficult to be fixed directly to the testing machine. So in order to protect the films from tearing, one piece of adhesive tape is used to connect the film to some small metal sheet, and then a thin nylon thread is used to connect the metal sheet to the testing machine. As the nylon thread is one meter long and the crosshead displacement is not more than 30 mm, the change of the peel angle during peel test is not more than $\arctan(0.03) \approx 1.5°$, so the peel angle is kept approximately.

Fig. 2 Peel test rig made specifically for the current research.

It is also important to keep the velocity of the crack growth v_{crack} unchanged, i.e.

$$\frac{v}{1-\cos\Phi} = v_{\text{crack}} = \text{const} \tag{3}$$

Here v is the moving velocity of the crosshead and Φ is the peel angle. The constant is 1 mm/min in our peel tests.

2.2. Experimental Results

2.2.1. Materials

A. Film:

Firstly, the film is tested using the uniaxial tension and the stress-strain curve is fitted using the following piece power-law hardening relations

$$\sigma = \begin{cases} E\varepsilon & (\sigma \le \sigma_y) \\ \dfrac{\sigma_y}{(\sigma_y/E)^n}\varepsilon^n & (\sigma \ge \sigma_y) \end{cases} \tag{4}$$

where n is strain hardening exponent. Table 1 shows the material parameters of the Al films.

Table 1. **Material parameters of the Al films**

film thickness (μm)	Young's modulus* (GPa)	Poisson's ratio*	yield strength (MPa)	strain hardening exponent
20	71	0.31	36.3	0.238
50	71	0.31	34.0	0.243
80	71	0.31	33.2	0.246
100	71	0.31	32.8	0.249
200	71	0.31	32.0	0.251
225	71	0.31	31.9	0.250
250	71	0.31	31.8	0.250

$*$ From materials handbook.

B. Adhesive materials:

The stress-strain curves for both ductile and brittle adhesives are obtained also through the uniaxial tension test, and the results are shown in Fig.3. From Fig.3, the ductile and brittle adhesives have the

maximum stresses 12 MPa and 24 MPa, respectively, while they have the maximum failure strains 56% and 8.7%. From Figs.3(a) and (b), the stress-strain curves of both ductile and brittle adhesive materials have the maximum stress values. Two materials display plastic softing after obtaining the maximum stress. The softing feature of the adhesive materials will be used to determine the separation strength in the following §3.2.

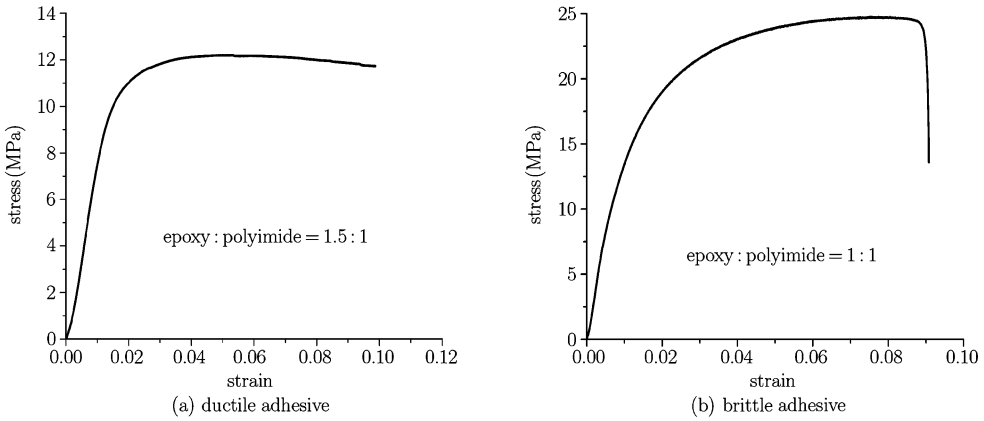

Fig. 3. Stress strain curves of the adhesive materials.

C. Material Al_2O_3 :

Substrate material, $Al_2O_3$is treated as an elastic material with Young's modulus $E = 350$ GPa and poisson's ration $\nu = 0.3$ in finite element simulations in the present research.

2.2.2. Peel test results

The curves of peel force vs. crosshead displacement are recorded during the peel tests. In Fig.4, some typical curves of peel force vs. crosshead displacement for the ductile adhesive case are shown. Figures 4(a) and (b) correspond to the film thickness 50 microns and 80 microns, respectively. From Fig.4, obviously the peel process mainly consists of two stages: pre-peeling and steady-state peeling. Steady-state peeling will be considered in the present research. Figure 5 shows the results for the case of brittle adhesive. The results are similar to that of ductile adhesive case. Comparing the results in Figs.4 and 5, the steady-state peel force corresponding to the ductile adhesive (mass ratio is 1.5) is about 4 times that of the brittle adhesive case.

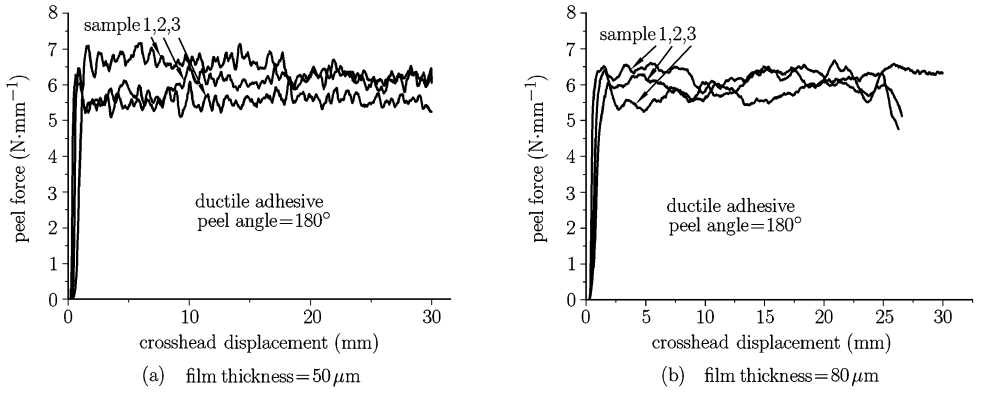

Fig. 4. Variations of the peel force with crosshead displacement for ductile adhesive case.

At least three samples are used in the peel tests for each film thickness and each peel angle. The mean value of the measured steady-state peel forces is taken as a function of the film thickness, and the

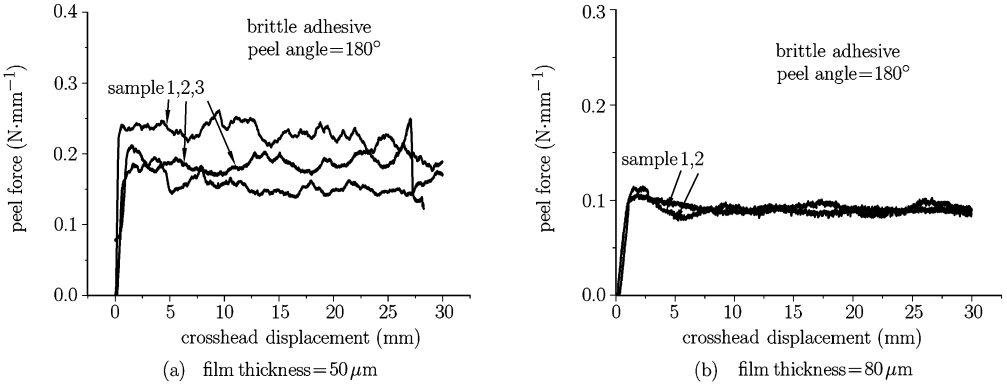

Fig. 5. Variations of the peel force with crosshead displacement for brittle adhesive case.

functions are plotted in Fig.6. The measured peel force in the ductile adhesive case is about $3 \sim 4$ times larger than that of the brittle adhesive case. For the ductile adhesive case, the steady-state peel force increases with increasing film thickness. However, for the brittle adhesive case, there exists a maximum value point along the peel force curve.

The adhesive layer thickness can be controlled by selecting different sizes of the SiO_2 spheres as introduced before. The steady-state peel force as a function of the adhesive layer thickness is plotted in Fig.7. For both kinds of adhesives the peel forces increase with increasing adhesive thickness until the stable values are reached.

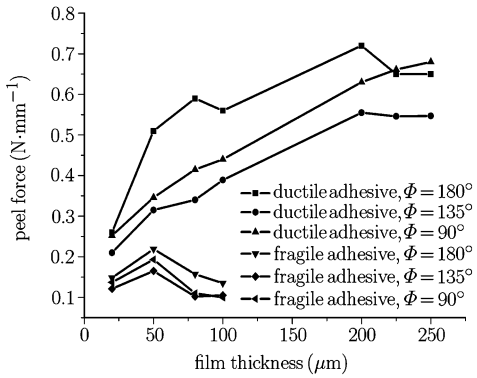

Fig. 6 Variations of the steady-state peel force *vs*. film thickness.

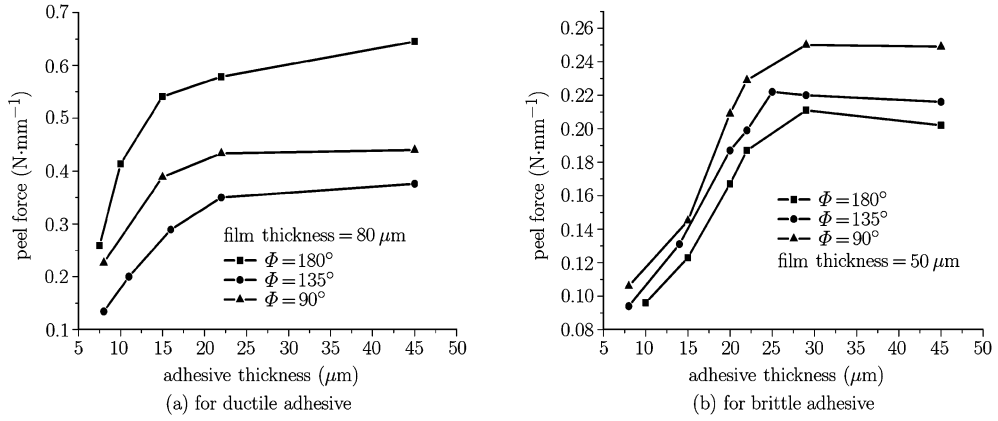

Fig. 7. Steady-state peel force *vs*. adhesive thickness.

III. FINITE ELEMENT SIMULATIONS

3.1. FE Model with the CZM

Since in the peel test the film width (10 mm) is much larger than its thickness ($20 \sim 250$ μm), the peel test problem can be treated as the plane strain case. The FE model using ABAQUS in version 6.5 is adopted. Equation (4) is used to characterize the stress strain relation of the Al film which will be treated as an elastic-plastic material. Large deformation, the von Mises yield criterion and isotropic

strain hardening will be considered in our FE model. The adhesive materials are also treated as an elastic-plastic case including the plastic softing, and material stress-strain relations are given in Fig.3. In the FE simulations, the data of stress-strain curves shown in Figs.3(a) and (b) are input for treating the plastic softing features by using ABAQUS version 6.5. Moreover, for substrate material, since the Al_2O_3 substrate undergoes the very small deformation during the peel tests, it can be treated as an elastic material with Young's modulus $E = 350$ GPa and poisson's ration $\nu = 0.3$. It is worth noting that since the film thicknesses we considered in the present research are not very small, we adopt the finite element program which is based on the conventional elastic-plastic theory. Otherwise the strain gradient finite element method should be used[27].

A single layer of CZ elements[3–5, 8–10, 15, 17] is employed to represent the adhesive layer. The interface parameters governing the traction separation law are the interface fracture toughness Γ_0, the separation strength $\hat{\sigma}$, the critical displacement ratio δ_n^c/δ_t^c and the factors λ_1 and λ_2, as described in Fig.1. Previous studies show that the shape of the traction separation law is relatively unimportant, and two independently important parameters are Γ_0 and $\hat{\sigma}$[5]. In our FE model we take $\lambda_1 = 0.15$, $\lambda_2 = 0.5$. The parameter δ_n^c/δ_t^c is important in the mixed mode fracture problems, but the predictions are relatively insensitive to this parameter as long as the fracture process is normal-separation dominant[28, 29], which is the case for the peel tests with the peel angle $90 \sim 180$ degrees considered in this paper.

For the convenience of exerting load on the film to simulate peel test, a rigid body is settled at the free end of the film. At first the free end of the film is rotated by the peel angle and then the film is peeled along this direction. The film and the substrate are meshed using bi-linear rectangular elements with four nodes and four integration points. The film undergoes large bending deformation during the peeling, so at least four layers of elements should be divided along the thickness of the film to capture large deformation information. Since Young's modulus of the substrate Al_2O_3 is about five times that of the Al film and the substrate undergoes small deformation during the peeling, a sparse mesh is adopted. Figure 8 shows a typical mesh used in our FE simulations. Four layers of elements are divided for the adhesive layer.

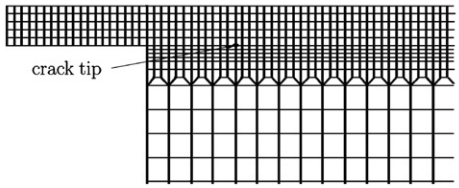

Fig. 8 A typical mesh used in the FE calculations.

3.2. Results and Discussions

3.2.1. Cohesive parameters Γ_0 and $\hat{\sigma}$

With the experimental stress-strain curves of the adhesives (Figs.3(a) and (b)), we can obtain the cohesive strength by recording and observing the variation of the near-tip normal stress (σ_{yy}) on the plane ahead of the crack tip (mean value of four integration points within the near-tip element) with loading steps. Figure 9 shows the result for the ductile adhesive case. The separation strength should be corresponding to the maximum stress value, $\hat{\sigma} = 24$ MPa. Similarly, we can also obtain $\hat{\sigma} = 37$ MPa for the brittle adhesive case. Once the separation strength $\hat{\sigma}$ has been obtained, one can further determine Γ_0. For one film thickness (50 μm) and one peel angle (90 degrees), Γ_0 can be identified by matching the simulated peel force with the experimental result. Figure 10 shows the variation of the peel force

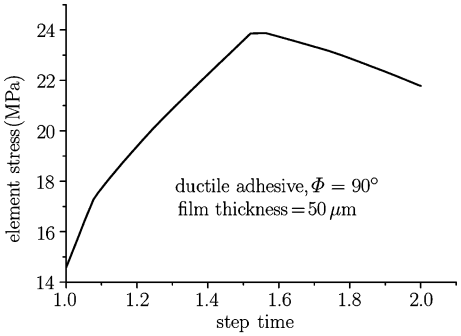

Fig. 9. The stress in the element at the crack tip varies as a function of the step time.

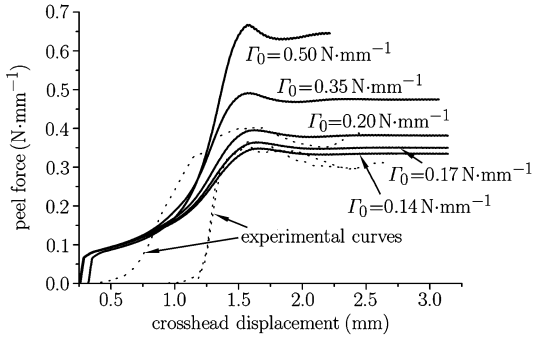

Fig. 10. Variation of the peel force *vs.* crosshead displacement for several Γ_0 values.

as a function of the crosshead displacement for a series of Γ_0 values. From Fig.10 we can obtain the fracture toughness $\Gamma_0 \approx 0.14$ N/mm for the ductile adhesive case, and $\Gamma_0 \approx 0.06$ N/mm for the brittle adhesive case.

3.2.2. Validation of the cohesive parameters

In order to validate the cohesive parameters obtained in the above §3.2.1, the peel tests with other film thicknesses and peel angles are predicted using the FE model with the above determined cohesive parameters. As for the ductile adhesive, Fig.11 shows the variation of the peel force as a function of the film thickness for various peel angles. The range of the experimental results is also shown. From Fig.11 it can be seen that the FE model captures the experimental results. It seems to conclude that the fracture toughness Γ_0 and the separation stress $\hat{\sigma}$ can be taken as the intrinsic interfacial parameters which are independent of the film thickness and the peel angle.

For brittle adhesive case, Fig.12 shows the variation of the peel force as a function of the film thickness for various peel angles. The range of the experimental results is also shown in the figure. From Fig.12 it also can be seen that the FE model captures the experimental features.

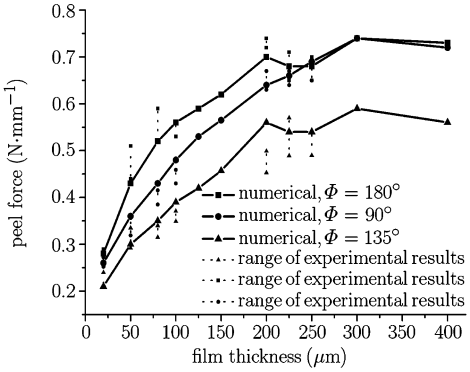

Fig. 11. The variation of the peel force as a function of the film thickness, for ductile adhesive.

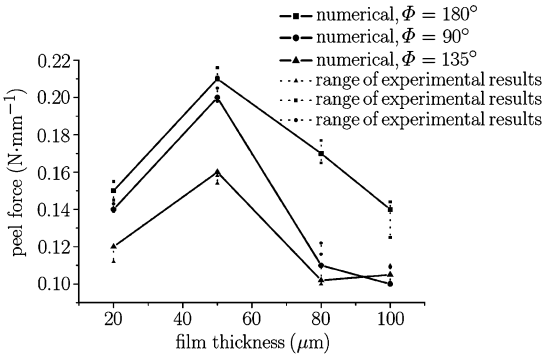

Fig. 12. The variation of the peel force as a function of the film thickness, for brittle adhesive.

3.2.3. The constraint effect of the adhesive layer thickness

From Fig.7 the fracture toughness Γ_0 is dependent on the thickness of the adhesive layer. The adhesive layer thickness considered in the above §3.2.1 is by default 20 μm. Using the method introduced in the above §3.2.1, one can obtain Γ_0 as a function of the adhesive layer thickness, shown in Figs.13(a) and (b). Γ_0 is comprised of two parts: the intrinsic work of interfacial fracture and the energy absorbed

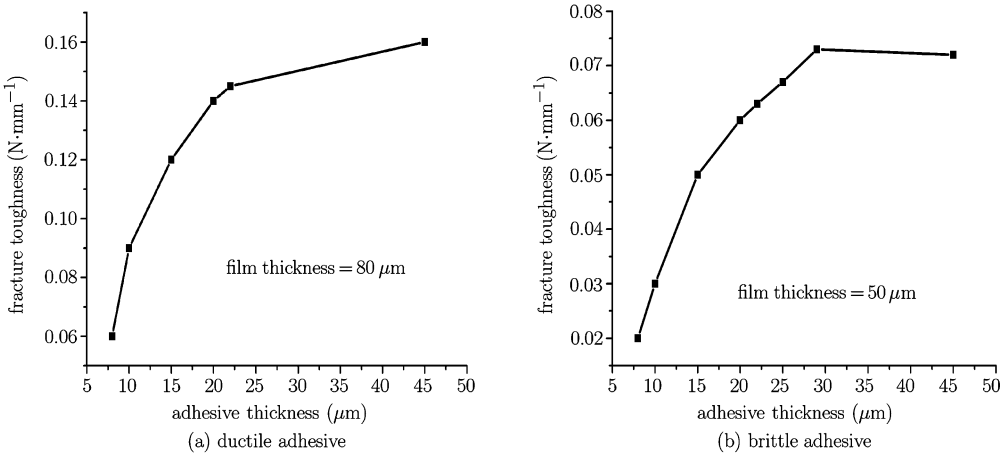

Fig. 13. The fracture toughness as a function of the adhesive layer thickness.

by the adhesive layer. When the adhesive layer exists, it undergoes plastic deformation and absorbs energy when the film is being peeled. So Γ_0 and P increase with increasing adhesive thickness, and they become insensitive to the adhesive thickness.

IV. CONCLUSION

Determination of interface mechanical properties for Al films along the ceramic substrate with different peel angles and different adhesive layers have been performed by using the peel test measurements and numerical simulations. A finite element model with the cohesive zone model is used to simulate the peel tests. With the help of the experimental stress-strain curves of the ductile and brittle adhesives, we have obtained the cohesive strength by simulating the stress variation near the crack tip. Furthermore, the cohesive energy Γ_0 has been identified by comparing the simulated peel force result with the experimental result. We have noted that from the present research, the finite element model can effectively capture the peel test features under steady-state peeling. Both cohesive energy Γ_0 and the separation strength $\hat{\sigma}$ can be taken as the intrinsic interfacial parameters which are independent of the film thickness and peel angle. However, they are dependent on the thickness of the adhesive layer. The constraint effect of the adhesive layer thickness is also discussed in the paper.

References

[1] Cotterell,B., Hbaieb,K., Williams,J.G., Hadavinia,H. and Tropsa,V., The root rotation in double cantilever beam and peel tests. *Mechanics of Materials*, 2006, 38: 571-580.

[2] Hadavinia,H., Kawashita,L., Kinloch,A.J., Moore,D.R. and Williams,J.G., A numerical analysis of the elastic-plastic peel test. *Engineering Fracture Mechanics*, 2006, 73(16): 2324-2335.

[3] Pardoen,T., Ferracin,T., Landis,C.M. and Delannay,F., Constraints effects in adhesive joint fracture. *Journal of the Mechanics and Physics of Solids*, 2005, 53: 1951-1983.

[4] Wei,Y., Thin layer splitting along the elastic-plastic solid surface. *International Journal of Fracture*, 2002, 113: 233-252.

[5] Wei,Y., Modeling nonlinear peeling of ductile thin films — critical assessment of analytical bending models using FE simulations. *International Journal of Solids and Structures*, 2004, 41: 5087-5104.

[6] Cui,J., Wang,R., Sinclair,A.N. and Spelt,J.K., A calibrated finite element model of adhesive peeling. *International Journal of Adhesion & Adhesives*, 2003, 23: 199-206.

[7] Song,J.Y. and Jin,Y., Analysis of the T-peel strength in a Cu/Cr/Polyimide system. *Acta Materialia*, 2002, 50: 3985.

[8] Yang,Q.D. and Thouless,M.D., Mixed-mode fracture analyses of plastically-deforming adhesive joints. *International Journal of Fracture*, 2001, 110: 175-187.

[9] Yang,Q.D., Thouless,M.D. and Ward,S.M., Numerical simulations of adhesively-bonded beams failing with extensive plastic deformation. *Journal of the Mechanics and Physics of Solids*, 1999, 47: 1337-1353.

[10] Yang,Q.D., Thouless,M.D. and Ward,S.M., Elastic-plastic mode-II fracture of adhesive joints. *International Journal of Solids and Structures*, 2001, 38: 3251-3262.

[11] Park,I.S. and Jin,Y., An X-ray study on the mechanical effects of the peel test in a Cu/Cr/Polyimide system. *Acta Materialia*, 1998, 46: 2947-2953.

[12] Park,Y.B., Park,I.S. and Jin,Y., Interfacial fracture energy measurement in the Cu/Cr/Polyimide system. *Materials Science & Engineering A*, 1999, 266: 261-266.

[13] Asai,H., Iwase,N. and Suga,T., Influence of ceramic surface treatment on peel-off strength between aluminum nitride and epoxy-modified polyaminobismaleimide adhesive. *IEEE Trans Adv Pack*, 2001, 24: 104-112.

[14] Bundy,K., Schlegel,U., Rahn,B., Geret,V. and Perren,S., Improved peel test method for measurement of adhesion to biomaterials. *Journal of Materials Science: Materials in Medicine*, 2000, 11: 517-521.

[15] Dillard,D.A. and Pocius,A.V., The Mechanics of Adhesion. Elsevier Press, 2002.

[16] Ferracin,T., Landis,C.M., Delannay,F. and Pardoen,T., On the determination of the cohesive zone properties of an adhesive layer from the analysis of the wedge-peel test. *International Journal of Solids and Structures*, 2003, 40: 2889-2904.

[17] Wei,Y. and Hutchinson,J.W., Interface strength, work of adhesion and plasticity in the peel test. *International Journal of Fracture*, 1998, 93: 315-333.

[18] Kim,K.S. and Aravas,N., Elasto-plastic analysis of the peel test. *International Journal of Solids and Structures*, 1988, 24: 417-435.

[19] Kinloch,A.J., Lau,C.C. and Williams,J.G., The peeling of flexible laminates. *International Journal of Fracture*, 1994, 66: 45-70.

[20] Kim,J., Kim,K.S. and Kim,Y.H., Mechanical effects of peel adhesion test. *Journal of Adhesion Science and Technology*, 1989, 3: 175-187.
[21] Wei,Y., Zhao,H. and Cao,A., Modeling and measurement of plastic dissipation in micron-thickness thin film peeling. The 12th International Symposium on Plasticity, Halifax, Canada, 2006, July 17-22.
[22] Moidu,A.K., Sinclair,A.N. and Spelt,J.K., Analysis of the peel test: prediction of adherend plastic dissipation and extraction of fracture energy in metal-to-metal adhesive joints. *Journal of Testing and Evaluation*, 1995, 23: 241-253.
[23] Moidu,A.K., Sinclair,A.N. and Spelt,J.K., On the determination of fracture energy using the peel test. *Journal of Testing and Evaluation*, 1998, 26: 247-254.
[24] Wei,Y. and Zhao,H., Peeling experiments of ductile thin films along ceramic substrates — critical assessment of analytical models. *International Journal of Solids & Structures*, 2008, 45: 3779-3792.
[25] Zhao,H. and Wei,Y., Determination of interface properties between micron-thick metal film and ceramic substrate using peel test. *International Journal of Fracture*, 2007, 144: 103-112.
[26] Zhao,H. and Wei,Y., Inverse analysis to determine interfacial properties between metal film and ceramic substrate with an adhesive layer. *Acta Mechanica Sinica*, 2008, 24: 297-303.
[27] Wei,Y., A new finite element method for strain gradient theories and applications to fracture analyses. *European Journal of Mechanics A/Solids*, 2006, 25: 897-913.
[28] Tvergaard,V. and Hutchinson,J.W., The influence of plasticity on mixed mode interface fracture. *Journal of the Mechanics and Physics of Solids*, 1993, 41: 1119-1135.
[29] Wei,Y. and Hutchinson,J.W., Nonlinear delamination mechanics for thin films. *Journal of the Mechanics and Physics of Solids*, 1997, 45: 1137-1159.